AD-A119 635 SRI INTERNATIONAL MENLO PARK CA F/G 7/4
INVESTIGATION OF MECHANISMS IN FIELD-DESORBED ION FORMATION USI--ETC(U)
AUG 82 S E BUTTRILL DAAG29-78-C-0034
UNCLASSIFIED ARO-15893.2-LS NL

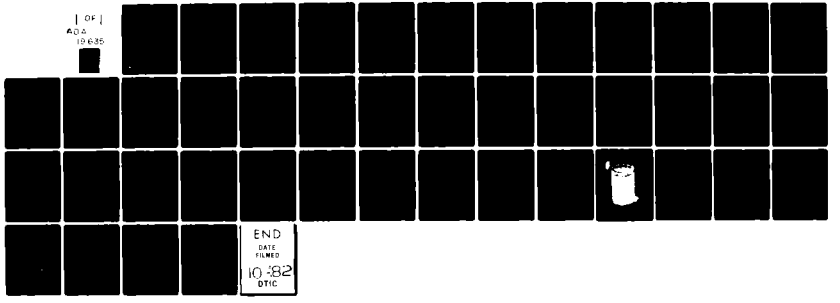

ARO 15893.2-LS

(12)

INVESTIGATION OF MECHANISMS IN FIELD-DESORBED ION FORMATION USING A PULSED FIELD DESORPTION TIME-OF-FLIGHT MASS SPECTROMETER

Final Technical Report

S. E. Buttrill, Jr.

August 1982

U. S. ARMY RESEARCH OFFICE
Post Office Box 12211
Research Triangle Park, NC 27709

Contract No. DAAG29-78-C-0034
SRI Project PYU-7707

SRI International
333 Ravenswood Avenue
Menlo Park, CA 94025

333 Ravenswood Ave. • Menlo Park, CA 94025
(415) 859-6200 • TWX: 910-373-2046 • Telex: 334 486

UNCLASSIFIED
SECURITY CLASSIFICATION OF THIS PAGE (When Data Entered)

REPORT DOCUMENTATION PAGE

READ INSTRUCTIONS BEFORE COMPLETING FORM

1. REPORT NUMBER	2. GOVT ACCESSION NO. AD-A119635
3. RECIPIENT'S CATALOG NUMBER	
4. TITLE (and Subtitle) INVESTIGATION OF MECHANISMS IN FIELD-DESORBED ION FORMATION USING A PULSED FIELD DESORPTION TIME-OF-FLIGHT MASS SPECTROMETER	5. TYPE OF REPORT & PERIOD COVERED FINAL TECHNICAL covering 15 Aug 78 thru 19 Nov 81
	6. PERFORMING ORG. REPORT NUMBER Final PYU-7707
7. AUTHOR(s) S. E. Buttrill, Jr.	8. CONTRACT OR GRANT NUMBER(s) DAAG 29-78-C-0034 Proj. P-15893-L
9. PERFORMING ORGANIZATION NAME AND ADDRESS SRI International 333 Ravenswood Ave. Menlo Park, CA 94025	10. PROGRAM ELEMENT, PROJECT, TASK AREA & WORK UNIT NUMBERS
11. CONTROLLING OFFICE NAME AND ADDRESS U. S. Army Research Office Post Office Box 12211 Research Triangle Park, NC 27709	12. REPORT DATE August 1982
	13. NUMBER OF PAGES 44
14. MONITORING AGENCY NAME & ADDRESS(if different from Controlling Office)	15. SECURITY CLASS. (of this report) Unclassified
	15a. DECLASSIFICATION/DOWNGRADING SCHEDULE

16. DISTRIBUTION STATEMENT (of this Report)

Approved for public release; distribution unlimited.

17. DISTRIBUTION STATEMENT (of the abstract entered in Block 20, if different from Report)

NA

18. SUPPLEMENTARY NOTES

The view, opinions, and/or findings contained in this report are those of the author(s) and should not be construed as an official Department of the Army position, policy, or decision, unless so designated by other documentation.

19. KEY WORDS (Continue on reverse side if necessary and identify by block number)

mass spectrometry, field ionization, field desorption, laser desorption, laser ionization, ionization mechanism, time-of-flight mass spectrometer

20. ABSTRACT (Continue on reverse side if necessary and identify by block number)

A pulsed field desorption time-of-flight mass spectrometer was designed and tested. Second-order energy focusing was achieved using a two-stage electrostatic reflector. Ions were formed by applying a 80-150 ns negative pulse of 2200 volts to a counter electrode spaced 50-200 micrometers away from either silicon or carbon activated emitters. The interaction of the high voltage pulse with the ion packet caused a large spread in the ion energy and limited mass resolution to only 400 at m/z 152. In separate experiments using a pulsed laser to produce ions, a time resolution of 1450 was obtained at m/z 242.

DD FORM 1 JAN 73 1473 EDITION OF 1 NOV 65 IS OBSOLETE

UNCLASSIFIED
SECURITY CLASSIFICATION OF THIS PAGE (When Data Entered)

INTRODUCTION

Of the numerous analytical tools now available for identifying and quantifying chemical substances, mass spectrometry is probably the most versatile and sensitive. For many analytical problems in biochemistry, bacteriology, and environmental studies, however, mass spectrometric methods are of limited effectiveness because the chemical or biological species to be measured are not volatile enough or are unstable when heated. It is well known that field desorption ionization provides a method of ionizing these difficult molecules without the necessity of vaporizing them first. The samples are placed directly on the field desorption emitter, and ionization occurs on the surface. However, before the technique can be used routinely, especially for quantitative measurements, more needs to be known about the factors relating the desorbed ion current to the nature and condition of the sample and to the conditions of operation of the field desorption source.

This project had two primary objectives. The first was to develop a pulsed field desorption time-of-flight mass spectrometer using an electrostatic mirror to obtain second-order focusing with respect to energy. The second objective was to use this mass spectrometer system to study the mechanism of field desorption, including the kinetics of ion formation following the onset of the imposition of the high electric field used for field desorption.

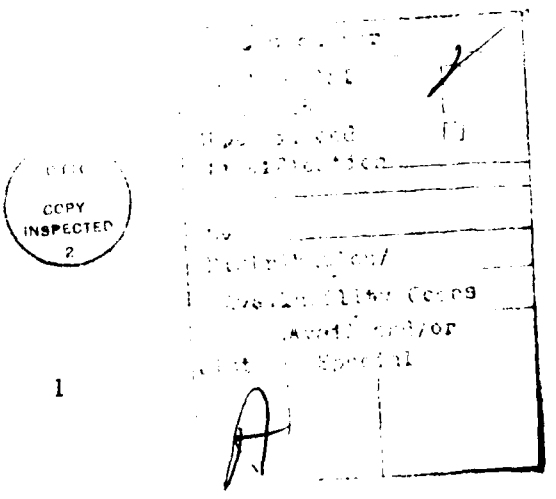

EXPERIMENTAL PROCEDURES

Pulsed Field Desorption

The pulsed field desorption time-of-flight mass spectrometer constructed for this project is described in detail in a paper accepted for publication in the International Journal of Mass Spectrometry and Ion Physics. A preprint of this paper is attached as the Appendix. The major features of this instrument are (1) a heated desorption probe that allows direct measurement of the temperature of the field desorption emitter during a pulsed field desorption experiment, (2) an electrostatic mirror that provides second-order energy focusing with respect to ion times of flight (after the design described by Mamyrin), and (3) a 40-mm-diameter multichannel plate detector.

The instrument can be operated in the field desorption mode, in which samples are placed directly on the silicon activated or carbon activated emitter. It can also be operated in the field ionization mode, in which the sample is introduced directly into the vacuum envelope of the mass spectrometer through a micrometering valve.

As described in the Appendix, the interaction of the ions formed by field desorption with the second half of the high voltage pulse produced a wide spread in ion energies, typically over 300 volts for a nominal ion energy of 1500 volts. Although the electrostatic reflector successfully compensated for much of this very wide energy spread, the limiting time-of-flight resolution at m/z 152 was only about 400. This large energy spread is unavoidable with the present design because the ion packet travels such a short distance during the 80-150 ns duration of the high voltage pulse.

Pulsed Laser Desorption

Because high voltage pulses were not capable of providing very short pulses of field desorbed ions of uniform energy, we were unable to conduct the planned studies of the time dependence of ion formation during the field desorption process. However, if the time-of-flight mass spectrometer is operated with only dc voltages, the instrument is capable of measuring the time dependence of other ion formation processes. We therefore took advantage of an opportunity to evaluate the use of a pulsed laser to produce narrow packets of ions for time-of-flight mass analysis. The laser was a Quanta-Ray DCR1 Nd:YAG laser, which has a 10-ns pulse width. The main beam of this laser has a wavelength of 1064 nm, and it was partially doubled to a wavelength of 532 nm in the green. The presence of the visible component in the beam greatly increased the convenience and safety of the experiments because it made the laser beam visible to the operator. No significant wavelength dependence of the pulsed laser desorption was found when these two wavelengths were compared.

In the pulsed laser mode of operation, the emitter was maintained at a constant potential of 1700 volts. A grounded grid was positioned approximately 120 μm from the emitter. The laser beam was directed and partially focused onto the emitter through the grid in near normal incidence (approximately 15°). The ions formed as a result of the laser pulse were rapidly accelerated to the grounded grid, focused by an Einzel lens, and deflected by two pairs of parallel plates into the electrostatic reflector located approximately one meter away. The multichannel plate detector was located directly above the ion source.

Many emitter materials were tried, including silicon-whisker-activated tungsten rods, polished tungsten rods, broken tungsten rods, gold-coated tungsten rods, gold-coated silicon-whisker-activated rods, silver alloy brazing rods, and silver-coated rods. All emitters gave similar results.

Spectra were recorded in two ways. At very low signal strength, it was possible to record time-of-flight spectra, using a time-to-amplitude converter (TAC) and a multichannel analyzer. In this experiment, the laser

trigger pulse served as the start pulse for the TAC and the detection of an ion at the multichannel plate served as the stop pulse. It was necessary to restrict this mode of data collection to very low signal strength because, on the average, fewer than one ion per laser pulse could be recorded without distorting the spectra.

The second mode of recording time-of-flight spectra was to photograph the screen of a 100-MHz storage oscilloscope. This method requires relatively large signals from each laser pulse, which were readily available.

RESULTS

Pulsed Field Desorption

The main experimental results from the pulsed field desorption experiments are described in the Appendix. Briefly, we found that the silicon-activated emitters of the rod geometry generally gave poor sensitivities in the pulsed field desorption mode for compounds such as arginine, adenosine, and sucrose. Very large signals could easily be observed for Li^+, Na^+, and K^+ at temperatures of 200°. In view of the previous good results obtained by other workers with silicon emitters in the normal ac FD configuration, our results suggest that the high electric field used in field desorption is important in the transport of molecules on the surface of the emitter to the active, field desorbing site.

The instrument was also tested in the field ionization mode of operation, in which methyl salicylate vapor was introduced into the mass spectrometer vacuum system. The field ionization signal went down as emitter temperature was increased. Nonetheless, the field ionization signal was much stronger than could be obtained for field desorption of polar organic compounds.

Taken together, the above results suggest the following picture for the field desorption process. The probability that a molecule will be ionized and subsequently field desorbed is proportional to the amount of time that the molecule spends on the field desorbing sites of the emitter. Sample molecules leave the emitter at high temperatures owing to normal thermal evaporation and/or decomposition. Molecules are transported to the field desorbing sites by both diffusion over the surface and, more important, by the attractive interaction between the permanent dipole of the molecule and the very high electric fields at the field desorbing sites. As emitter temperatures are increased, the mobility of the sample molecules

on the emitter surface increases. However, the rate of evaporation of the sample also increases. The completition between these two effects accounts for the well-known observation that for each compound there is a "best emitter temperature", or BET.

Laser Desorption Experiments

Two modes of ion formation could be obtained readily using the pulsed laser irradiation. At low laser powers, which were measured to be less than approximately 20 MW/cm^2, a phenomenon occurred that can be described as photodesorption of ionic species. Substances that normally exist in ionic form, such as salts of lithium, sodium, cesium, potassium, barium, and tetra alkyl ammonium compounds, are desorbed from the emitter during the laser pulse. Thousands of ions of these species were desorbed and detected for each laser pulse. Saturation of the multichannel plate detector was frequently observed when monitoring these ions at relatively low laser power.

At higher laser powers (greater than 20 MW/cm^2), a new phenomenon was observed. At these powers, the very large ion currents produced threatened to overload the multichannel plate detector. The duration of these ion pulses exceeded 100 μs, the normal observation time in our experiments.

We believe that the source of these large, persistent ion currents is a surface plasma formed on the emitter. At the higher laser powers, electrical breakdown of the emitter surface occurs, and the resulting plasma is opaque to the laser radiation. When breakdowns occur during the early part of the laser pulse, essentially all the subsequent energy is completely absorded. In contrast, the major fraction of the laser energy is reflected when electrical breakdown does not occur on the emitter surface.

This model accounts for the observed very rapid changeover from photodesorption to the plasma mode of ion formation with increasing laser power. Changing the laser power by less than a factor of two completely changes the mode of ion formation from photodesorption to surface plasma.

Because of the very long duration of the surface plasma ion process and the very large ion signals produced, very few experiments were performed in this mode of operation. Even though time-of-flight mass analysis was not possible for these persistent ion currents, it was noticed that with sucrose as a sample a large signal did begin at approximately the arrival time for the quasi-molecular ion of sucrose.

Operation of the time-of-flight mass spectrometer with pulsed laser desorption of ionic species at relatively low laser powers allowed us to demonstrate the high mass resolution expected from the electrostatic reflector configuration. The tetraethyl ammonium ion at m/z 242 could be recorded on the 100-MHz storage oscilloscope with a full width at half height of only 50 ns. The arrival time of this peak was 72.67 ms, which gives a time resolution of 1450. For a constant peak width in time, the mass resolution of the time-of-flight mass spectrometer increases as the square root of the ion mass. Therefore, these results indicate the potential for unit mass resolution at masses over 2000 using the present time-of-flight mass spectrometer configuration. The desirability of using the ion reflector principle with other methods of pulsed ion formation, such as plasma desorption, is apparent.

The photodesorption of ionic species appeared to be confined to substances that are clearly present on the emitter surface in ionic form. Several experiments were attempted in which samples of sucrose, arginine, and adenosine with various salts were tested at low laser power. In all but one case, we failed to observe any detectable molecular ion. In one case, using the multichannel scaler and TAC, it was possible to record a weak spectrum of sucrose. This experiment was quite difficult, however, because of the tendency of the system to slip over into the surface plasma mode of ion formation.

PUBLICATIONS AND TECHNICAL REPORTS

1. "Pulsed Field Desorption Mass Spectrometry," by R. W. Odom and S. E. Buttrill, Jr, presented at the 27th Annual Conference on Mass Spectrometry and Allied Topics, Seattle, Washington, June 3-8, 1979.

2. "A Pulsed Field Desorption Time-of-Flight Mass Spectrometer," by S. E. Buttrill, Jr., R. H. Fleming, M. Rossi, W. Gohl, and L. N. Goeller, presented at the 29th Conference on Mass Spectrometry and Allied Topics, Minneapolis, Minnesota, May 24-29, 1981.

3. "Pulsed Field Desorption Mass Spectrometry: A Technique for Investigating Field Desorption Ion Formation Mechanisms," by R. W. Odom, S. E. Buttrill, Jr., R. H. Fleming, M. Rossi, L. N. Goeller, and W. Gohl, International Journal of Mass Spectrometry and Ion Physics, accepted for publication.

4. "Laser Desorption Time-of-Flight Mass Spectrometry," by S. E. Buttrill, Jr., and R. H. Fleming, in preparation.

PARTICIPATING SCIENTIFIC PERSONNEL

S. E. Buttrill, Jr., Ph.D., Principal Investigator

Robert W. Odom, Ph.D.

Ronald H. Fleming, Ph.D.

Michel J. Rossi, Ph.D.

Wolfgang Gohl

Larry N. Goeller

CONCLUSIONS

The results of this research demonstrate that the pulsed field desorption technique is valuable for investigating the formation of ions from molecules adsorbed on surfaces. The coupling of the pulsed laser desorption technique with time-of-flight mass analysis demonstrates that field ionization does not occur as gaseous sample molecules pass through the high field region near FD-FI emitters. The incorporation of the ion reflection technique enhances the mass resolution of the time-of-flight mass analysis to the extent that ion arrival time widths are direct indications of ion formation time, and it maintains the high ion collection efficiency characteristic of time-of-flight mass analysis. Silicon emitters produced satisfactory results in field ionization experiments.

Appendix

PULSED FIELD DESORPTION MASS SPECTROMETRY: A TECHNIQUE FOR INVESTIGATING FIELD DESORPTION ION FORMATION MECHANISMS

R. W. Odom, S. E. Buttrill, Jr., R. H. Fleming,
M. Rossi, L. N. Goeller, and W. Gohl

SRI International, Menlo Park, CA 94025

ABSTRACT

Field desorption mass spectra of thermally labile compounds are readily obtained using a new pulsed field desorption (PFD) time-of-flight (TOF) mass spectrometer. Ions are formed by applying a short high voltage pulse to the cathode of a field desorption source. The resolution of the subsequent TOF mass analysis is significantly increased by incorporation of an electrostatic reflector into the ions flight path. The spectra of methyl salicylate, perylene, arginine, and adenosine are discussed in terms of the predominant ionization mechanisms occurring under PFD conditions.

INTRODUCTION

Since its introduction as an analytical technique in 1969 (1), field desorption mass spectrometry (FDMS) has been increasingly applied (2-6) to the mass analysis of nonvolatile and thermally labile compounds. The primary reason for this increased application of the field desorption (FD) ionization technique is that it provides a method for directly ionizing molecules adsorbed on a surface and results in minimal thermal decomposition of the adsorbed neutrals. According to the original theory of field desorbed ion formation (7), subjecting the adsorbed molecules to a high ($> 10^7$ V/cm) electric field sufficiently distorts the potential energy surfaces of the neutral and ionic states that electron transfer from the molecules to the FD emitter can occur. The positive ions formed on the surface are subsequently repelled and thus desorbed by the electric field.

Field desorption is a term normally applied only to molecules already present on the emitter surface usually as a result of deposition from solution. Field ionization is the term used when the molecules are supplied via the gas phase onto the field anode. Two mechanisms are possible for field ionization: first, physical adsorption of the sample onto the emitter followed by field desorption, and second, tunneling of an electron from the sample into the emitter as the gaseous molecules pass through the high field region near the emitter (3). For purposes of discussing ionization mechanisms, we will include field ionization by adsorption-field desorption in the same category as simple field desorption. Furthermore, we will use

the term "surface reaction" for those field desorption processes in which the ion is formed by addition of a preexisting cation (such as H^+, Na^+, K^+) to an adsorbed neutral molecule or by fragmentation of an adsorbed ion.

Since ion formation under field desorption conditions typically results in very small amounts (~ 0.1 eV) (5) of excitation energy being transferred to the ion, ion fragmentation reactions are often negligible. Both the small degree of thermal decomposition and minimal ion dissociation processes result in mass spectra characterized by ion signals at or near the mass of the neutral precursor molecule and fragment ion signals which result from simple bond cleavages. Thus, field desorbed mass spectra typically permit direct determinations of the molecular weights of molecules which would undergo extensive decomposition and/or fragmentation if it were necessary to vaporize the molecules before ionization as is required in electron impact (EI), chemical ionization (CI), and field ionization (FI) techniques.

Numerous examples of successful application of FDMS to analysis of compounds of biological and environmental importance are in the literature. The analysis of natural products such as sugars (9), nucleosides and nucleotides (10), amino acids (11) and peptides (12), drugs and metabolites (13), and pesticides (14) are examples where FDMS has provided mass identification as well as structure and sequence information. Despite the growing number of successful applications, the FD method of generating mass spectra requires a high degree of operator skill, often exhibits poor reproducibility in repetitive determinations, and frequently does not produce ions from neutrals which should readily ionize under FD

conditions. In addition, it has been recognized since the onset (1) of analytical FDMS investigations that surface reactions play a major, if not dominant, role in the types of ions formed. The formation of protonated molecular ions $(MH)^+$, dimers [M_2^+ or $(M_2H)^+$], and higher cluster ions, as well as the well documented cationization (15) process [formation of $(MA)^+$ complexes where A is an alkali atom] are experimental evidence for the predominance of surface reactions on the FD emitter. Recently, Holland and coworkers (16) have proposed that surface reactions are the dominant ionization mechanisms observed in most FDMS studies. The role of the electric field between the FD anode and cathode (or counter electrode) according to these investigators is only to reduce the activation energy for these surface reactions and assist in extracting and focusing the ions formed on the surface.

We recently initiated a research program designed to determine the principle mechanisms contributing to ion formation under nominal field desorption conditions. The initial goals of this research program were to design an FD mass spectrometric system which had the ability to distinguish field ionization, field desorption and surface reaction (ionization) processes. The system we developed is a pulsed field desorption (PFD) time-of-flight (TOF) mass spectrometer. In operation, packets of ions are formed from molecules adsorbed on the FD emitter by applying short (50-150 ns) high voltage pulses (up to -2.2 kV) to the cathode of an FD source. Mass analysis of the ions is obtained from their time-of-flight from source to detector. The mass resolution of

this system is significantly enhanced compared to conventional TOF mass analysis techniques by incorporating an ion reflection system originally developed by Mamyrin et al. (17).

The concept of producing field desorbed ions by applying short, high voltage pulses to a FD source originated with the initial investigations of field evaporation processes (18-20) in which singly and multiply charged metal ions are desorbed from a metallic emitter. Subsequent investigations (21-26) of the surface reactions of molecules adsorbed on to FD emitters from the gas phase have established the value of the PFD technique for determining the mechanisms of proton transfer, catalysis and polymerization reactions. The PFD technique, however, has not been applied previously to studies of field desorbed ion formation from non-volatile, thermally labile compounds. In this paper we discuss the design and performance of the mass spectrometer and present several representative spectra of molecules desorbed from the surface of an FD emitter. These mass spectra are discussed in terms of the predominant mechanism affecting ionization and are compared to the spectra obtained under continuous field desorption conditions.

EXPERIMENTAL

A schematic of the TOF apparatus is shown in Figure 1 and consists essentially of the following components:

1. An FD source (emitter and 80% transmission screen counter electrode) with a vacuum lock for introducing the probe (emitter holder) into the vacuum system and a micrometer adjustment for positioning the emitter with respect to the counter electrode. Following the counter electrode there is a grounded 80% transmission grid.

2. Ion focusing and deflection electrodes consisting of a cone shaped (4.4 mm long, 6.3 mm O.D. and 2.8 mm I.D.) focusing electrode, two sets of electrostatic quadrupole lenses (27) and a pair of vertical deflection plates. In some experiments, a set of vertical and a set of horizontal deflection plates following an Einsel lens were used.
3. 1 m flight path between the source and the ion reflector. The ion beam is deflected approximately 2° from the horizontal by the quadrupole lens and vertical deflection plates. This separates the ion beam from fast neutrals formed in the source and permits positioning the ion detector directly above the source.
4. Ion reflector consisting of two deceleration stages. The kinetic energy of the ion beam is reduced to about 30% of its initial value in the first decelerating stage, and the beam is stopped and its direction of travel reversed in the second stage. The reflected ion beam then returns through the 1 m drift space to the ion detector (channel electron multiplier, Galileo Electro-Optics Corp. Sturbridge, MA, model 4700) located above the source. In some experiments a multichannel plate electron multiplier was used.

The high voltage pulses which generate packets of field desorbed ions are produced by a high power pulse generator (Cober Electronics, Inc., Stamfort, CT, model 605 P), and the synchronous trigger pulses from this unit are used to initiate the timing sequence of the detection electronics. These trigger pulses are fed to a variable delay pulse generator (Ortec, Inc., Oak Ridge, TN, model 416 A) which initiates a start pulse on a time to pulse height converter (TPHC, Ortec, model 457). The delay between the high voltage pulse and the start

of the TPHC is set at 5 μs or more which is sufficient time to suppress any pickup of the counter electrode high voltage pulse by the electron multiplier. The stop pulses to the TPHC are provided by the amplified detected ion pulses arriving at the multiplier. A histogram (ion counts versus ion arrival time) is accumulated by storing the TPHC output voltage pulses in a 4096 channel multichannel analyzer (Ortec, model 6240) operated in a pulse height analysis mode. The stored arrival time spectrum can be printed on a Teletypewriter, plotted on an X-Y recorder, and manually converted to a mass spectrum by identifying two known masses in the spectrum or by running a calibration spectrum. Since the pulsed mode ion detection rate is typically much less than one ion count per high voltage pulse (pulse frequencies between 8-10 kHz), discrimination against higher mass ions is not significant with this detection system.

As mentioned above, the reflector enhances the mass resolution of TOF mass analysis. The ion reflection technique results in second order time focusing of the ion beam with respect to ion energy so that the time spread in the flight time of ions at a particular mass is simply their formation time spread. The expression for the mass resolution of the TOF analysis reduces to

$$M/\Delta M = t/2\Delta t \qquad (1)$$

under these conditions, where t is the total flight time and Δt is the width of the ion formation pulse.

The ion reflector used in our mass spectrometer is shown in Figure 2. Its design is based on the original description of the ion reflection technique presented by Mamyrin et al. (17). The ion deflector is approximately 15.2 cm in overall length and was constructed by stacking 12.1 cm O.D. by 9.53 cm

I.D. stainless steel plates (0.38 mm thick) on six ceramic rods. The length of the two-stage deceleration and reflection lens is determined by the overall field free flight path of the ions ($\ell_1+\ell_2$ = L in Figure 1) which for our system is 2 m. The initial deceleration stage consists of two plates spaced 1.6 cm apart (d_D in Figure 1). This length is approximately 0.008 L. These two plates are covered with a 98% transmission nickel grid in order to maintain field uniformity between the plates. The reflection stage of this lens consists of seventy plates spaced 80.4 μm apart using ceramic washers, and its overall length is 12.2 cm (d_R in Figure 1). This length is approximately 0.06 L. The necessary uniform electric field in the reflection stage is achieved by a string of resistors (100 kΩ) extending from the back mounting plate to the decelerating plate. A 1.27 cm hole was drilled in the center of the back mounting plate and a channel electron multiplier was positioned about 0.63 cm behind this plate. This auxiliary multiplier (Galileo, model 4700) permits tuning the source ion optics for maximum ion transmission into the reflector when the deceleration and reflection voltages are off.

Most of the mass spectra discussed in this paper were obtained using activated (carbonaceous dendrites) tantalum foils (38.1 μm thick). However, an emitter system based on the silicon whisker production technique of Matsuo and coworkers (28) was also evaluated. The emitters themselves were constructed from tungsten posts (12.7 mm x 1.59 mm) that were polished flat using Emory No. 600 paper followed by Emory 4/0 polishing paper. The tungsten posts were ultrasonically cleaned in water and methanol, and a layer of gold was vacuum deposited on the flat surface. An array of the tungsten rods was placed in a stainless steel heater block equipped with a thermocouple.

The block was heated to 630°C in an atmosphere of argon (250 torr). The chamber was quickly evacuated, power to the heater was reduced, and 5% silane in 95% argon (200 torr) was introduced. By this time the thermocouple read 620°C. A mat of silicon whiskers was produced within 30 s, silane and argon were pumped out, and the heater was allowed to cool to room temperature.

A direct inlet probe (Figure 3) was constructed to accept the silicon whiskered tungsten posts. The probe was provided with a heater, a thermocouple, and a micrometer for adjusting the emitter-to-counter electrode distance. The counter electrode consisted of a nickel grid with lines spaced every 0.1 mm (80% transmission). The emitter to counter electrode spacing was approximately 0.025 mm for the carbon emitters and 0.150 mm to 0.250 mm for the silicon emitters. Both carbon and silicon emitters were operated at +1.2 kV (V_o). Thus the ions nominally have 1.2 kV of kinetic energy in all of the field free regions of the flight tube. The amplitude of the high voltage counter electrode pulses was typically -2.0 to -2.2 kV. A dc bias of +0.3 to 0.6 kV was applied to the counter electrode to reduce ion desorption between pulses. The voltages on the ion reflector were typically 0.7 V_o and 1.15 V_o for the deceleration and reflection stages (V_D and V_R in Figure 1), respectively. The mass scale was calibrated by bleeding acetone, xylene or methyl salicylate vapor (pressure $\tilde{=}$ 0.10×10^{-6} torr) into the source chamber, and recording calibration spectra. The carbon emitters were heated indirectly by resistive heating of the source housing, and the temperature of the emitter was determined using a thermocouple mounted in close proximity to the copper emitter holder.

RESULTS AND DISCUSSION

The initial experiments performed with this apparatus were directed toward evaulating its performance with regard to reflected ion collection efficiency, sensitivity and mass resolution. The molecules used in these evaulations were methyl salicylate (introduced from the gas phase) and perylene (dilute solution placed directly on the emitter). Although these molecules have sufficient vapor pressure to be field ionized near the emitter, our results indicate that the primary ionization mechanism under pulsed field conditions is field desorption or field induced surface reactions.

Methyl salicylate (M.W. = 152) was used to determine the reflected ion collection efficiency of the TOF apparatus. This efficiency was determined by operating the system in a continuous mode, i.e., by applying a dc voltage of -1.7 kV to the counter electrode and measuring the ion signal collected at the multiplier behind the reflector with the reflection voltages off. The reflection voltages were then turned on and the reflected ion signal was collected on the detector multiplier. With a pressure of about 1×10^{-6} torr of methyl salicylate in the apparatus, the unreflected ion signal was typically between 2×10^{5} and 3×10^{5} counts per second. The magnitude of this signal seemed to depend primarily on the condition of the emitter (age and extent of activation). With the reflection voltages on, the ion signal collected at the detector varied between 1.6 and 3.0×10^{4} counts per second which yields a reflected ion collection efficiency of 8 to 10% of the ions entering the reflector.

An example of the mass resolution obtained with our apparatus is shown in Figure 4, which is an expanded arrival time spectrum of the M^+ and $(M+1)^+$ ions of methyl salicylate. The ion formation pulses applied to the counter electrode were 150 ns wide (full width at half maximum, FWHM), the peak pulse voltage was -2.0 kV (120 ns wide at the peak), and the pulse repetition rate was 8.3 kHz. The emitter temperature was 60°C. This spectrum was accumulated for 400 s and the intensity of the M^+ and $(M+1)^+$ ion represent about 10% of the total collected ion signal. The mass resolution was calculated to be 277 using the FWHM of the M^+ peak at Δt. Resolution using silicon emitters was typically 240-280.

Several experiments help to establish which factors are important in determining the resolution of the apparatus. Note that the flat disk-shaped ion packet produced by the silicon emitters is well suited to the geometry of the TOF mass spectrometer. Nevertheless, instrument resolution did not depend significantly on the emitter (silicon on tungsten rods or carbon on tantalum foil). The emitter to counterelectrode distance (0.025 to 0.250 mm) also had little effect. Several variations of focus element shape and spacing failed to produce significant improvement in resolution. Since ions can strike the cathode over a 3-4 mm distance along the axis of a continuous dynode electron multiplier, a distribution in the flight paths of the ions and thus the arrival time of the secondary electrons at the anode of the multiplier could conceivably be observed. However, substitution of a (flat) multichannel plate type electron multiplier (Galileo 3040-B-00MMA) for the original channel electron multiplier showed that this was not the limiting factor in determining resolution. The shapes of the M^+ peaks were also observed to be

essentially constant as the pulse width was increased from 50 to 200 ns and it was only at the 400 ns setting that the peak exhibited noticeable broadening as illustrated in Figure 5 for methyl salicylate.

The main factor which limited instrument resolution proved to be variability in ion energy. In a series of experiments with methyl salicylate, a peak width at half height of 160 ns was observed using 140 ns high voltages pulses. A "hard" reflector consisting of a grid at +1500 V (V_D) was used to reflect the ions back to the detector without energy focusing. Using a 140 ns pulse width, the full width at half height of the M^+ peak was 3.8 μs and the mean arrival time was 54.9 μs. This peak has a wide bottom; full width at 10% height was 13.4 μs. The peak width corresponds to an energy spread of 13.2% at half height and 24.7% at 10% height. Based on the theory of electrostatic reflectors (17) and the geometry of our particular instrument, we expected energy spreads of about 10% to be adequately focused. In an experiment with the "hard" reflector using 500 ns high voltage pulses, the full width at half height was only 9.7%.

From these experiments we have drawn three conclusions:

1. The electrostatic reflector successfully compensates for much of the wide energy spread.
2. However, the wide energy spread is ultimately the limiting factor in instrument resolution.
3. The source of the high energy spread is the interaction of the ion packet with the pulse itself. This is largely unavoidable because ions travel such a short distance during the 50 to 200 ns duration of the pulse. With longer pulse duration, most of the ions are in the field free region before the pulse turns off.

Those ions which have not reached the grounded grid by the time the pulse ends have more than 1200 eV of kinetic energy. This is because the region between the counter electrode and the grounded grid accelerates ions after the pulse ends. Ions with less than 1200 eV of kinetic energy are formed because of the finite rise time (∿15 ns) of the pulse. As the high voltage pulse width increases, the fraction of ions with too much or too little energy decreases. Thus TOF mass spectra acquired with longer pulse widths are less affected by energy spreads too wide to be focused.

The longest high voltage pulse width (400 ns) used to acquire the spectra in Figure 5 produced a peak (m/z 152) consisting of an ion "burst" followed by a long "tail" to later arrival times. A relatively large number of ions are apparently formed at the beginning of each pulse. During long pulses the rate of formation of ions falls off and approaches a constant level. This level reflects the rate at which sample is supplied to the active regions of the emitter. The rate controlling supply step might be migration of adsorbed molecules over the emitter surface from an inactive region to an active region, or the slow step might be resupply of sample to the emitter from the gas phase. A mechanism in which ions are formed as gas phase sample molecules pass near the emitter is not consistent with the initial ion burst. The data in Figure 5 suggest that 50 and 100 ns pulses do not deplete the active emitter sites and that 200 ns pulses are just beginning to cause sample depletion.

The overall sensitivity of the pulsed field desorption technique was determined using perylene as the sample compound. Approximately 100 ng of perylene dissolved in toluene was placed on the emitter and the mass spectrum was obtained at an emitter temperature of 100°C. The potential on the emitter

and reflector as well as the amplitude, duration and repetition rate of the counter electrode pulses were the same as those used in the methyl salicylate spectrum in Figure 4. The complete mass spectrum for perylene is shown in Figure 6. In addition to intense signals observed at the M^+ and $(M+1)^+$ positions of the perylene ion, we observe a number of ions with masses below ~ 100. The most intense of the majority of these lower mass ions are spaced 14 mass units apart and are attributed to the presence of hydrocarbons on the emitter. These peaks are always present when emitters activated with carbon dendrites are used. They are not observed using silicon on tungsten emitters. The FWHM of the M^+ peak of perylene is 127 ns which corresponds to a resolution of 275 [Eq. (1)], essentially the same resolution observed in the methyl salicylate spectrum. The M^+ and $(M+1)^+$ peaks are not completely resolved because of the tailing of the M^+ peak. The sum of the ion counts in the M^+ and $(M+1)^+$ peaks is 3.38×10^4 which constitutes 6.2% of the total ion counts for the spectrum. The sensitivity of the PFD-TOF system for perylene is calculated to be 1.4×10^{-10} ions/molecule (5.4×10^{-14} coulomb/μg) which compares favorably to the sensitivity reported for commercially available FDMS systems. Using silicon emitters, 6.4×10^3 ions were produced from 100 ng perylene (2.7×10^{-11} ion/molecule).

To demonstrate the application of the pulsed field desorption technique to the analysis of thermally labile compounds, we obtained the mass spectra of samples of the amino acid arginine and the nucleoside adenosine. With regard to arginine, ions characteristic of the intact amino acid are not observed under EI, CI or FI conditions (14, 29), although quasi-molecular ions can be obtained with FD, rapid heating, and plasma desorption

techniques (11, 30, 31). This compound is therefore a good test sample for checking the performance of the PFD technique and comparing the mass spectra obtained under pulsed conditions with continuous FD mass spectra.

The complete PFD mass spectrum of arginine is shown in Figure 7, and this same spectrum expanded about the 150 to 200 amu range is shown in Figure 8. This spectrum was obtained in 400 s from a sample of approximately 100 ng of arginine placed on a carbon emitter. The width of the counter electrode pulses was 150 ns (FWHM) and the emitter temperature was approximately 200°C. The other experimental conditions were the same as those discussed above for methyl salicylate and perylene. The complete mass spectrum (Figure 6) shows that the major ions resulting from arginine are the $(MH)^+$ ion at mass 175 and $(MH)^+ - NH_3$ ion at mass 158. These two ions constitute 1.5% of the total ion counts for this spectrum. Ions produced by cationization of arginine by Na^+ are evident at m/z 197: $(MNa)^+$ and 180: $(MNa)^+ - NH_3$. In addition to the low mass hydrocarbon background present with carbon emitters, the arginine spectrum has intense signals at masses 23 and 39 (base peak) corresponding respectively to desorption of Na^+ and K^+ from the emitter. Since this is the only PFD spectrum in which these ions were observed, either the sample solution was contaminated with sodium and potassium salts, or the efficiency of field desorption was unusually high for this emitter. Considering the expanded mass spectrum (Figure 8), the FWHM time spread of the major peaks is approximately 120 ns from which the mass resolution at the $(MH)^+$ peak is calculated to be 250. The other ion signals at m/z values higher than the $(MH)^+$ ion are probably the result of cationization reactions of the sodium and potassium ions with arginine on the emitter surface.

The relative intensities of the ion signals originating from arginine obtained under pulsed and continuous FD (11) conditions are compared in Table 1. It is quite apparent from this table that the arginine molecule undergoes significantly less fragmentation in the PFD mode indicating that less energy is deposited in the molecule during ionization. This lower degree of excitation in the pulsed experiment may either be the result of the lower emitter temperature used in the PFD work (200 C° versus 220°C for the continuous spectrum) or the reduced extent of negative ion bombardment of the emitter under the pulsed conditions.

Both the pulsed and continuous FD spectra of this compound indicate that surface reactions, in particular proton transfer, are the major ion formation processes. This is clearly evident in the expanded PFD spectrum (Figure 8) which shows a total absence of the $M^{+\cdot}$ ion of arginine.

The PFD mass spectrum of adenosine is illustrated in Figure 9. This spectrum was obtained from a 100 ng sample with the same experimental conditions used in obtaining the arginine spectrum. The $M^{+\cdot}$ and $(MH)^+$ ions are the major adenosine peaks in this spectrum and constitute about 4.4% of the total ion count. The FWHM time width of the $(MH)^+$ base peak is 150 ns resulting in a mass resolution of 230. A comparison of the relative ion intensities obtained for this molecule with the pulsed and continuous FD (2) techniques is given in Table 2. It appears that the main differences in the respective relative intensities are related to differences in surface reactions. For example, the presence of the signal at mass 237 in the pulsed spectrum may result from loss of the CH_2OH radical from surface protonated adenosine, or by loss of formaldehyde from surface bound $M^{+\cdot}$. The resulting ion would then be desorbed from the emitter, possibly leaving the CH_2OH group

or CH_2O bound to the surface. The signal at mass 31 $(CH_2OH)^+$ could then result from either protonation of surface bound formaldehyde or loss of an electron from surface bound CH_2OH radical followed by desorption of $(CH_2OH)^+$. Thus it is possible that <u>both</u> fragments could appear as ions.

The peaks at m/e 134 and 135, $(C_5H_{10}O_4)^{+\cdot}$, and $(C_5H_5N_5)^{+\cdot}$ respectively, might also arise by way of surface reactions from two ions both of which are fragments of the same original molecule.

CONCLUSIONS

The results presented in this paper demonstrate that the pulsed field desorption technique is valuable for investigating the formation of ions from molecules adsorbed on surfaces. The coupling of the PFD technique with time-of-flight mass analysis demonstrates that field ionization does not occur as gaseous sample molecules pass through the high field region near FD-FI emitters. The incorporation of the ion reflection technique enhances the mass resolution of the TOF mass analysis to the extent that ion arrival time widths are direct indications of ion formation time, and it maintains the high ion collection efficiency characteristic of TOF mass analysis. Silicon emitters produced satisfactory results in FI experiments.

ACKNOWLEDGMENTS

This research was supported by the Army Research Office under Contract No. DAAG29-78-C-0034.

REFERENCES

1 H. D. Beckey, Int. J. Mass Spectrom. Ion Phys., 2 (1969) 500.

2 H. D. Beckey and H. R. Schulten, Angew Chem. Int. Edit. Engl., 14 (1975) 403.

3 H. D. Beckey, Principles of Field Ionization and Field Desorption Mass Spectrometry (Pergamon, London, 1977).

4 A. L. Burlingame, C.H.L. Shackleton, I. Howe, and O. S. Chizhov, Anal. Chem., 50 (1978) 346R.

5 H. D. Beckey, K. Levsen, F. W. Röllgen, and H. R. Schulten, Surf. Sci., 70 (1978) 325.

6 W. D. Reynolds, Anal. Chem., 51 (1978) 284A.

7 R. Gomer, Field Emission and Field Ionization (Harvard University Press, Cambridge, 1961).

8 T. C. Clements and E. W. Müller, J. Chem. Phys., 37 (1962) 2684.

9 H. R. Schulten and D. E. Games, Biomed. Mass Spectrom., 1 (1974) 120.

10 H. R. Schulten and H. D. Beckey, Org. Mass Spectrom., 7 (1973) 861.

11 H. U. Winkler and H. D. Beckey, Org. Mass Spectrom., 6 (1972) 655.

12 H. R. Schulten, Methods of Biochemical Analysis, Vol. 24, ed. D. Glick (Wiley Interscience, New York, 1977).

13 H. R. Schulten, Biomed. Mass Spectrom., 1 (1974) 223.

14 H. M. Fales, G.W.A. Milne, H. U. Winkler, H. D. Beckey, J. N. Damico, and R. Barron, Anal. Chem., 47 (1975) 207.

15 F. W. Röllgen and H. R. Schulten, Z. Naturforsch., 30a (1975) 1685.

16 J. F. Holland, B. Soltmann, and C. C. Sweely, Biomed, Mass. Spectrom., 3 (1976) 340; J. F. Holland, B. Soltmann, J. L. Dye, American Society for Mass Spectrometry 26th Annual Conference on Mass Spectrometry and Allied Topics, St. Louis, MO, 1978, Paper TA11.

17 B. A. Mamyrin, V. I. Karataev, D. V. Shmikk, and V. A. Zagulin, Sov. Phys.-JETP, 37 (1973) 45.

18 M. G. Inghram and R. Gomer, Z. Naturforsch., 10a (1955) 863.

19 E. W. Miller, J. A. Panitz, and S. B. Melane, Rev. Sci. Instrum., 39 (1968) 83.

20 P. J. Turner and M. J. Southon, Dynamic Mass Spectrometry, Vol. 1, Ch. 10, eds. D. Price and J. E. Williams (Heyden and Son, London, 1969).

21 J. H. Block, Z. Physik. Chem. (Frankfurt), 39 (1963) 169.

22 F. W. Röllgen and H. D. Beckey, Surf. Sci., 23 (1970) 69.

23 F. W. Röllgen and H. D. Beckey, Int. J. Mass Spectrom. Ion Phys., 12 (1973) 465.

24 F. W. Röllgen and H. D. Beckey, Z. Naturforsch., 29a, (1974) 230.

25 F. W. Röllgen, K. Levsen, and H. D. Beckey, Org. Mass Spectrom., 10 (1975) 737.

26 D. L. Cocke and J. H. Block, Surf. Sci., 70 (1978) 363.

27 C. S. Lu and H. E. Carr, Rev. Sci. Instrum., 33 (1962) 823.

28 T. Matsuo. H. Matsuda, and I. Katakuse, Anal. Chem., 51 (1979) 69.

29 P. A. Lecleroq and D. M. Desiderio, Org. Mass. Spectrom., 7 (1973) 515.

30 R. J. Beuhler, E. Flannigan, L. J. Greene, and L. Friedman, J. Am. Chem. Soc., 96 (1974) 3990.

31 D. F. Hunt, J. Shabanowitz, F. K. Botz, and D. A. Brent, Anal. Chem., 49 (1977) 1160.

Table 1

Comparison of the Relative Ion Intensities of Pulsed and Continuous FD Mass Spectra of Arginine

Fragment	Mass	Relative Intensity	
	(m/z)	PFD	Continuous FD (11)
$(MH)^+ - (CH_4N_3)^\cdot$	117	0	30
$(MH)^+ - NH_3$	158	49	100
$(MH)^+$	175	100	27

Table 2

Comparison of the Relative Ion Intensities of Pulsed and Continuous FD Mass Spectra of Adenosine

Mass (m/z)	Fragment	Relative Intensity	
		PFD	Continuous FD (2)
31	$(CH_2OH)^+$	48	15
32	$(CH_3OH)^{+\cdot}$	0	8
133	$(C_5H_9O_4)^+$	27	80
134	$(C_5H_{10}O_4)^{+\cdot}$	23	0
135	$(C_5H_5N_5)^{+\cdot}$	15	7
237	$(MH)^+ - (CH_2OH)\cdot$	24	0
267	$M^{+\cdot}$	69	100
268	$(MH)^+$	100	98

FIGURE CAPTIONS

Figure 1 Schematic diagram of pulsed field desorption mass spectrometer illustrating the flight path of ions from the source to detector. (The amplifier-discriminator is an Ortec, model 9302).

Figure 2 Photograph of the ion reflector showing the deceleration and reflection stages and the resistor string extending from the back plate to the decelerator plate.

Figure 3 Probe for use with silicon emitters. Note that the inner and outer Vespel portions are connected to a metal rod and tube respectively with o-ring vacuum seals.

Figure 4 Expanded PFD arrival time spectrum of the M^+ and $(M+1)^+$ ions of methyl salicylate. The mass resolution of the M^+ peak is calculated from Δt.

Figure 5 Expanded PFD arrival time spectrum of the M^+ and $(M+1)^+$ ions of methyl salicylate obtained with four different settings of the counter electrode pulse width.

Figure 6 PFD mass spectrum of perylene used for sensitivity calculation. Lower mass peaks in the spectrum are attributed to hydrocarbon impurities on the emitter.

Figure 7 PFD mass spectrum of arginine illustrating the peaks at $(MH)^+$ and $(MH)^+ - NH_3$ as well as the intense signals at m/z = 23(Na^+) and m/z = 39(K^+).

Figure 8 Expanded PFD mass spectrum of arginine over the mass range between 150 and 200 amu.

Figure 9 PFD mass spectrum of the nucleoside adenosine.

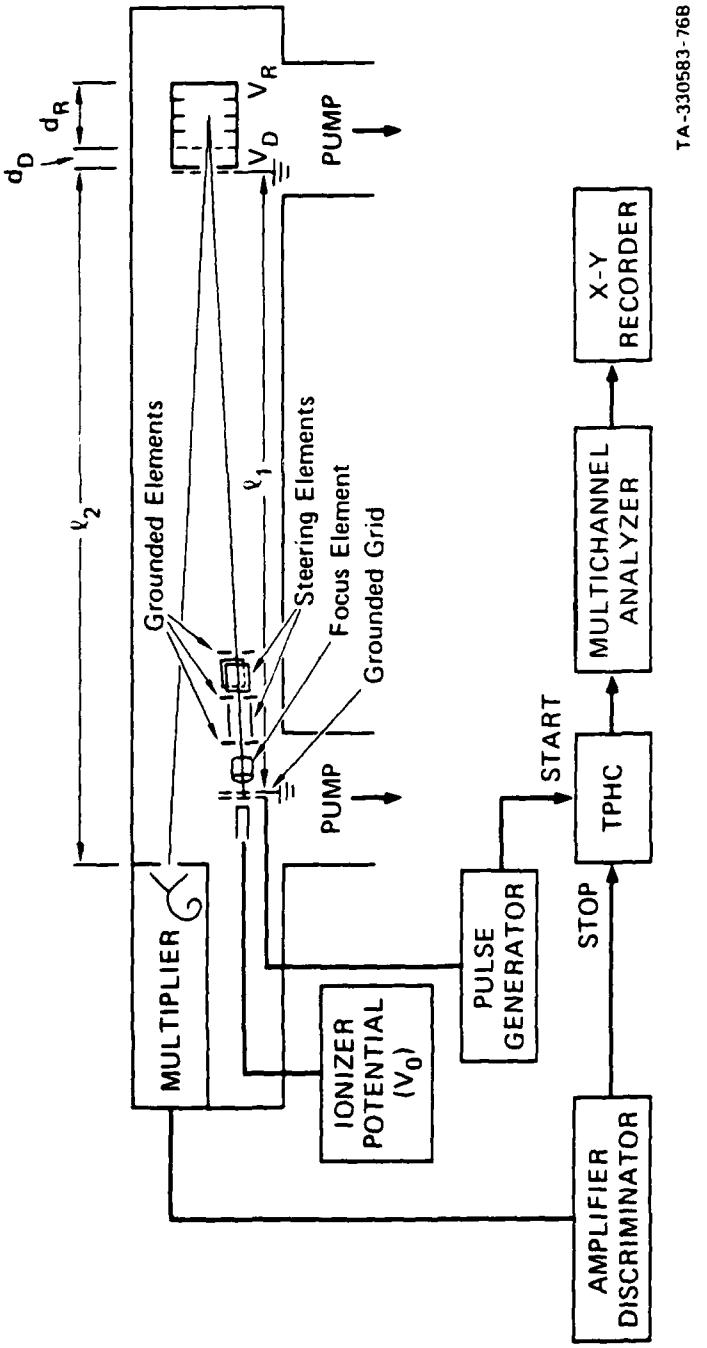
d_D
d_R
ℓ_2
ℓ_1
V_R
V_D
PUMP
Grounded Elements
Steering Elements
Focus Element
Grounded Grid
PUMP
MULTIPLIER
IONIZER POTENTIAL (V_0)
PULSE GENERATOR
START
STOP
TPHC
MULTICHANNEL ANALYZER
X-Y RECORDER
AMPLIFIER DISCRIMINATOR
TA-330583-76B

Figure 1

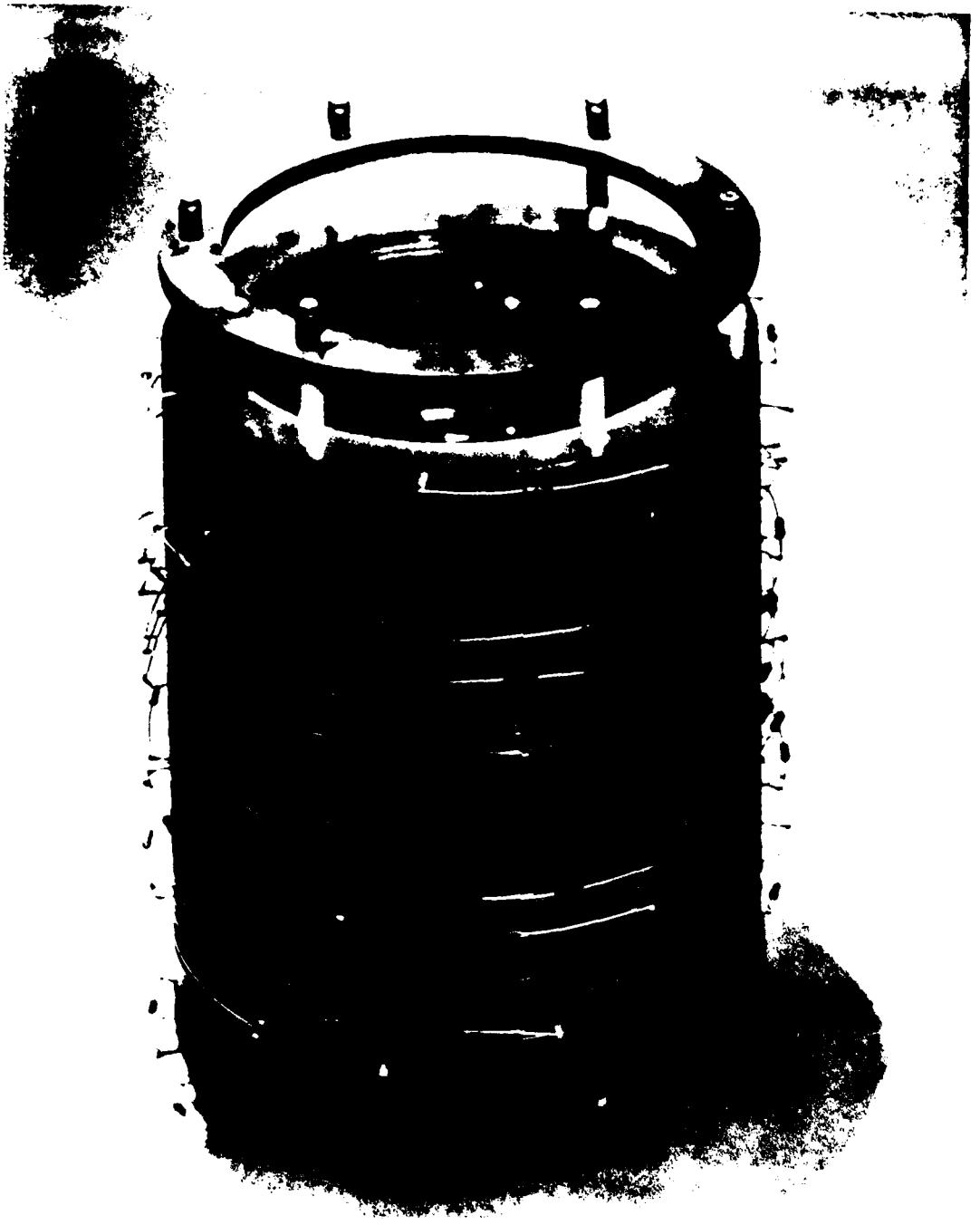

SA-7707-1

Figure 2

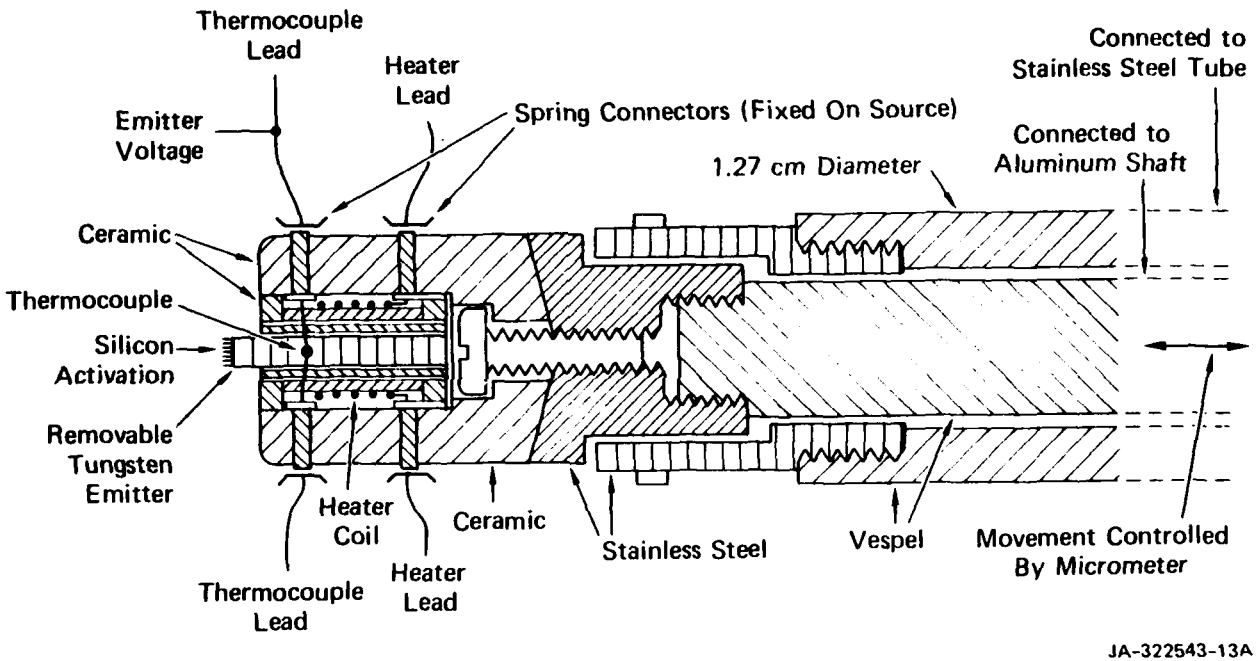
Thermocouple Lead
Heater Lead
Emitter Voltage
Spring Connectors (Fixed On Source)
Connected to Stainless Steel Tube
Connected to Aluminum Shaft
1.27 cm Diameter
Ceramic
Thermocouple
Silicon Activation
Removable Tungsten Emitter
Heater Coil
Ceramic
Stainless Steel
Vespel
Movement Controlled By Micrometer
Thermocouple Lead
Heater Lead
JA-322543-13A

Figure 3

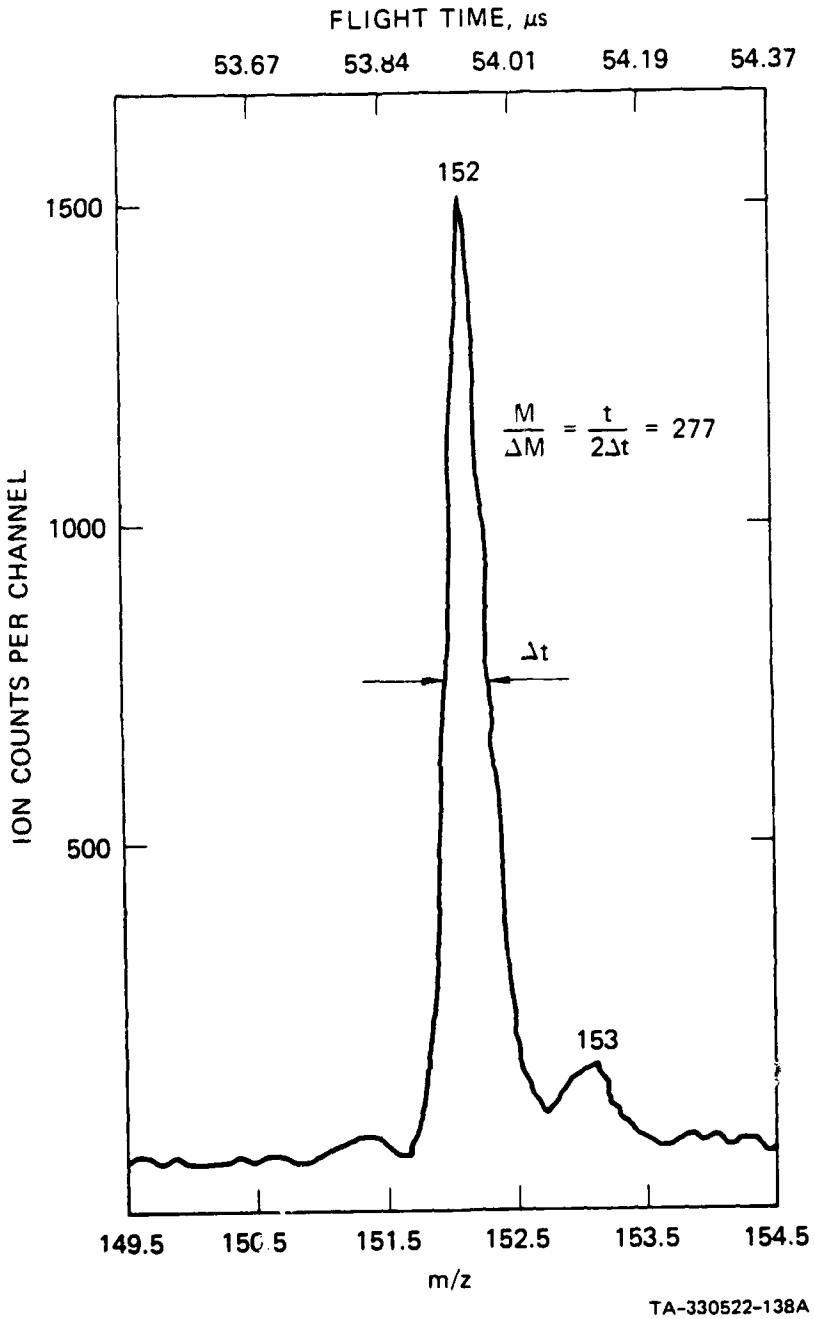
FLIGHT TIME, μs
53.67
53.84
54.01
54.19
54.37
152
1500
1000
500
ION COUNTS PER CHANNEL
M/ΔM = t/2Δt = 277
Δt
153
149.5
150.5
151.5
152.5
153.5
154.5
m/z
TA-330522-138A

Figure 4

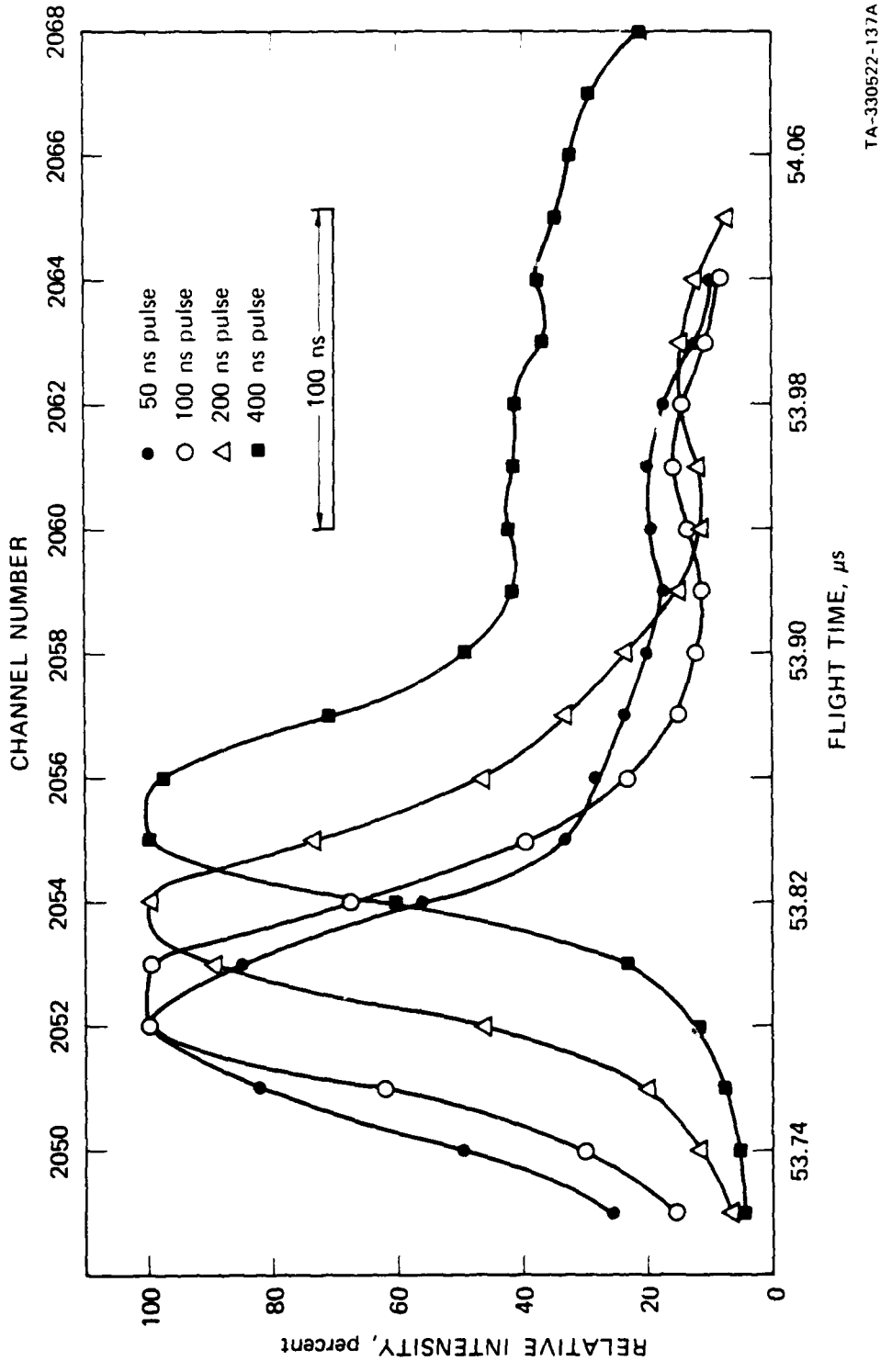
CHANNEL NUMBER
2050
2052
2054
2056
2058
2060
2062
2064
2066
2068
RELATIVE INTENSITY, percent
0
20
40
60
80
100
FLIGHT TIME, μs
53.74
53.82
53.90
53.98
54.06
50 ns pulse
100 ns pulse
200 ns pulse
400 ns pulse
100 ns
TA-330522-137A

Figure 5

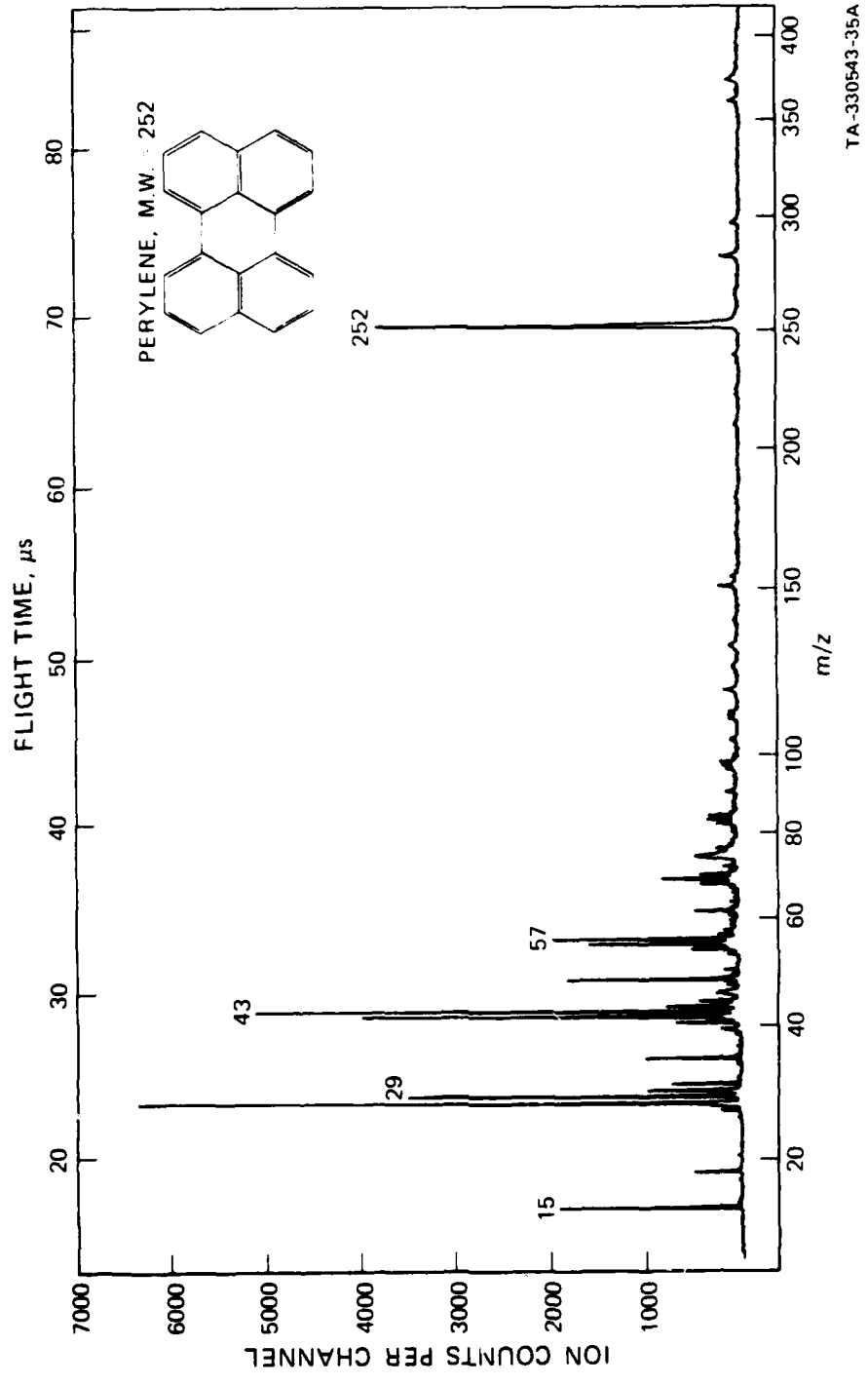
PERYLENE, M.W. = 252
252
57
43
29
15
ION COUNTS PER CHANNEL
7000
6000
5000
4000
3000
2000
1000
FLIGHT TIME, μs
20
30
40
50
60
70
80
m/z
20
40
60
80
100
150
200
250
300
350
400
TA-330543-35A

Fiugre 6

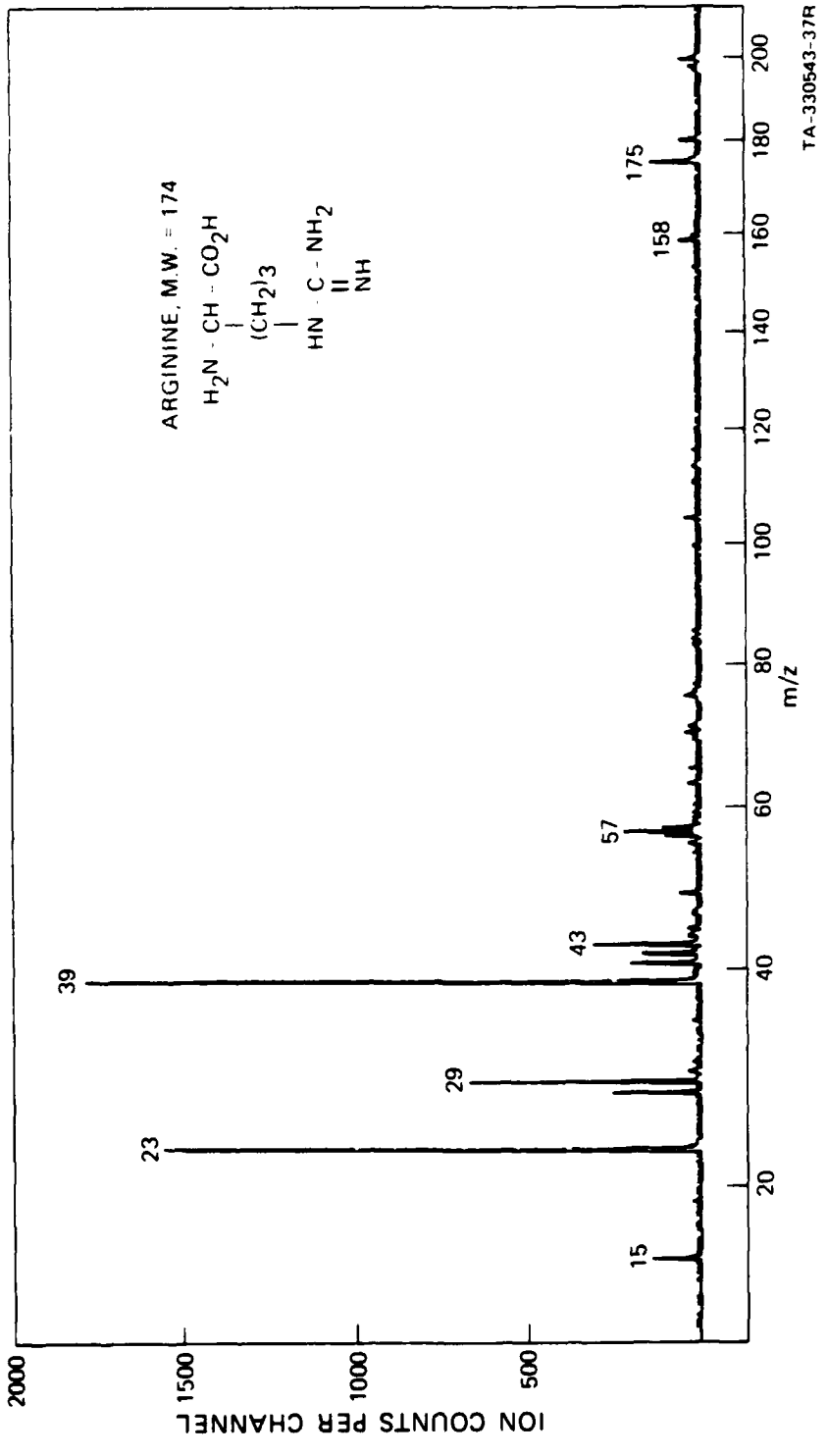
ARGININE, M.W. = 174
$H_2N - CH - CO_2H$
$(CH_2)_3$
$HN - C - NH_2$
NH
ION COUNTS PER CHANNEL
2000
1500
1000
500
m/z
20
40
60
80
100
120
140
160
180
200
15
23
29
39
43
57
158
175
TA-330543-37R

Fiugre 7

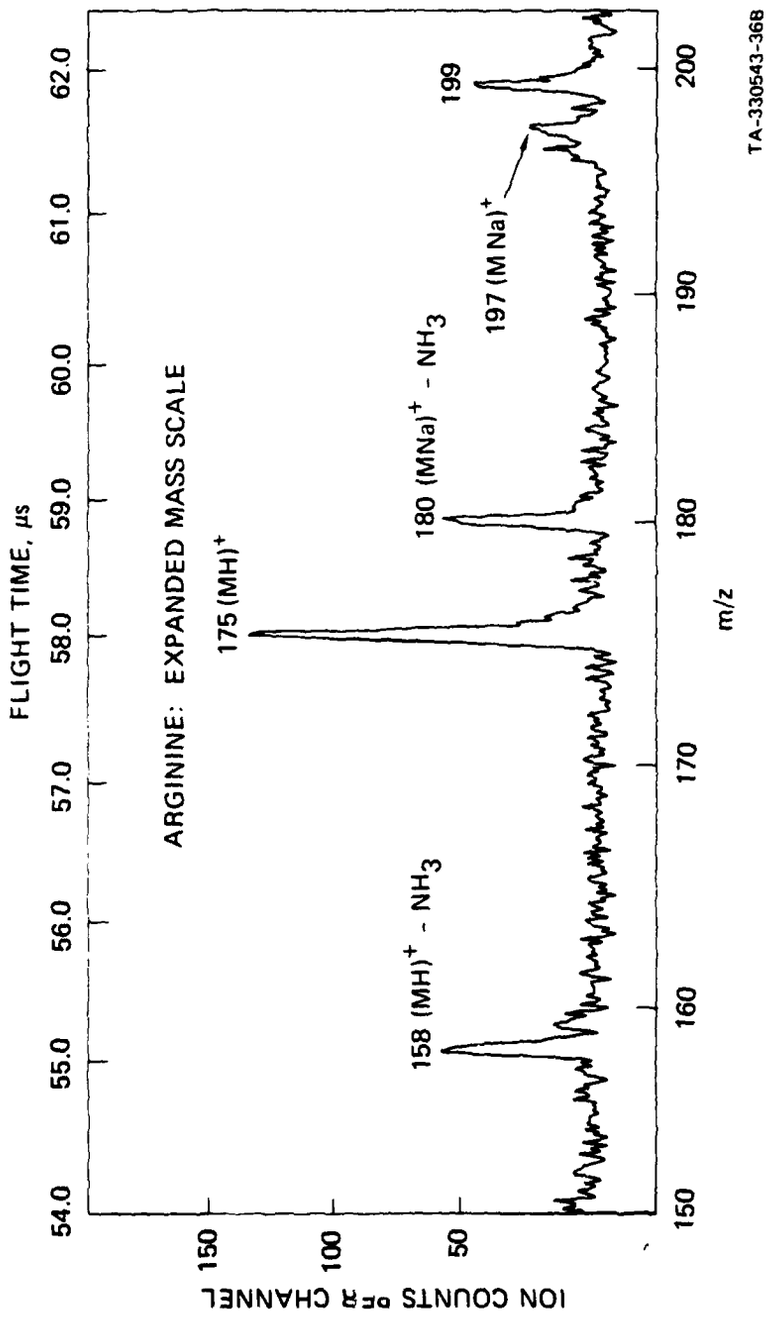
ARGININE: EXPANDED MASS SCALE
FLIGHT TIME, μs
54.0
55.0
56.0
57.0
58.0
59.0
60.0
61.0
62.0
ION COUNTS PER CHANNEL
150
100
50
158 (MH)+ - NH3
175 (MH)+
180 (MNa)+ - NH3
197 (M Na)+
199
150
160
170
180
190
200
m/z
TA-330543-36B

Figure 8

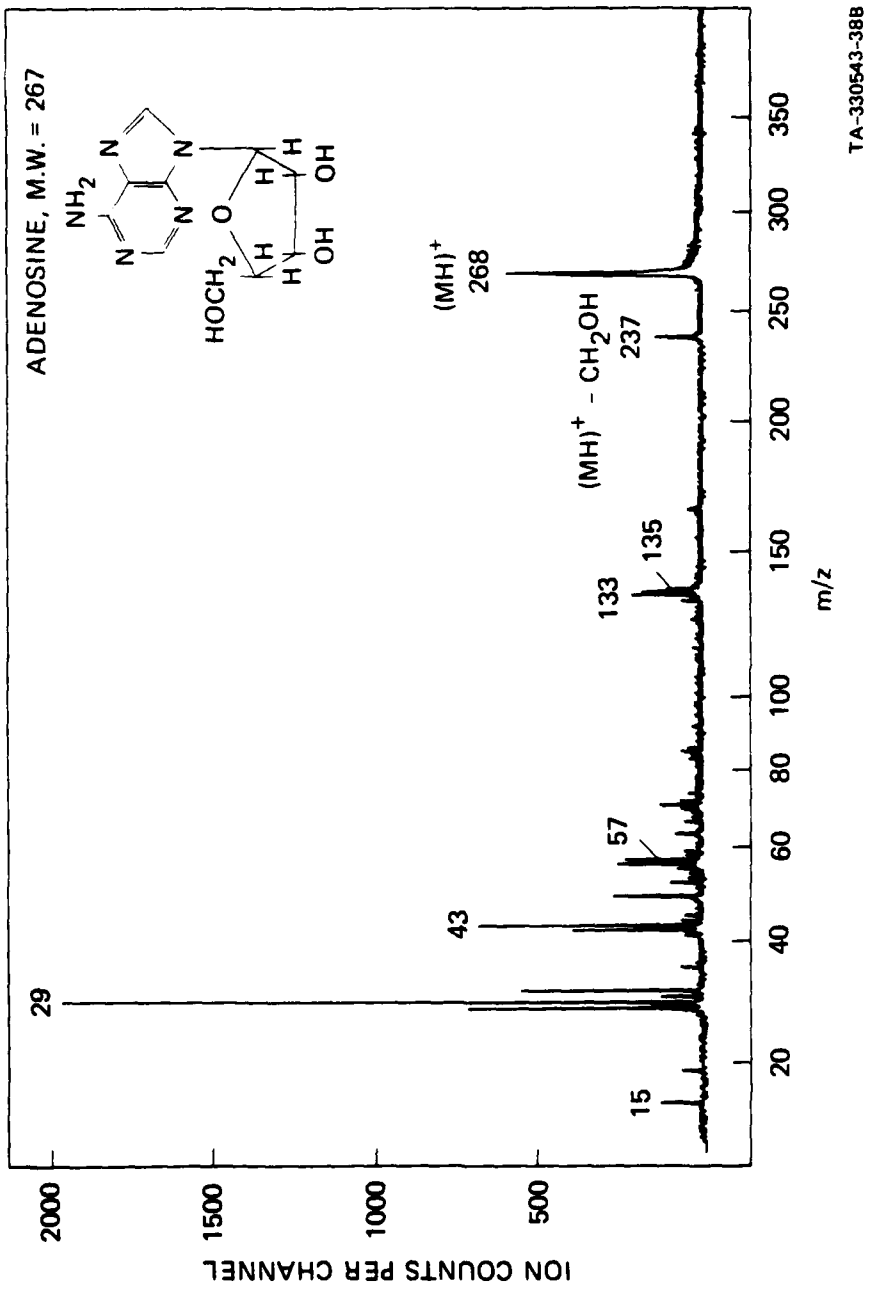
ADENOSINE, M.W. = 267
NH2
HOCH2
OH OH
(MH)+
268
(MH)+ - CH2OH
237
133
135
43
57
29
15
ION COUNTS PER CHANNEL
2000
1500
1000
500
20
40
60
80
100
150
200
250
300
350
m/z
TA-330543-38B

Figure 9

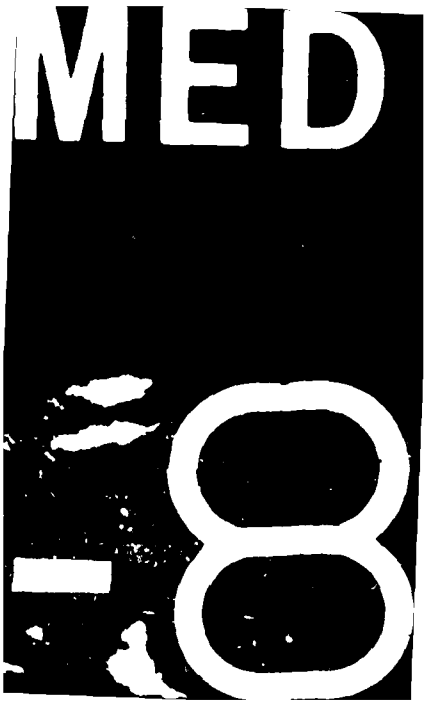
MED
8